J Mater Sci (2010) 45:2228–2232
DOI 10.1007/s10853-009-4117-0

HTC2009

Convectional controlled crystal–melt interface using two-phase radio-frequency electromagnetic heating

R. Hermann · G. Gerbeth · J. Priede · A. Krauze · G. Behr · B. Büchner

Received: 19 May 2009 / Accepted: 5 December 2009 / Published online: 22 December 2009

Abstract The radio frequency floating-zone growth of massive intermetallic single crystals is very often unsuccessful due to an unfavourable solid–liquid interface geometry enclosing concave fringes. This interface depends on the flow in the molten zone. A tailored magnetic two-phase stirrer system has been developed which enables the controlled influence on the melt flow ranging from intense inwards to outwards flows. Depending on the phase shift between the two induction coils, a transition from a double vortex structure to a single vortex structure is created at a preferable phase shift of 90°. This change in the flow field has a significant influence on the shape of the solid–liquid interface. Due to their attractive properties for high temperature applications such as high melting temperature, low density, high modulus and good oxidation resistance, the magnetic system was applied to the crystal growth of TiAl alloys.

R. Hermann (✉) · G. Behr · B. Büchner
Leibniz Institute of Solid State and Materials Research IFW Dresden, Mail-box 270016, 01171 Dresden, Germany
e-mail: r.hermann@ifw-dresden.de

G. Gerbeth
Forschungszentrum Dresden-Rossendorf, MHD Department, Mail-box 510119, 01314 Dresden, Germany

J. Priede
Applied Mathematics Research Centre, Department of Mathematical Sciences, Coventry University, Priory Street, Coventry CV1 5FB, UK

A. Krauze
Institute of Physics, University of Latvia, LV-2169, Salaspils Miera 32, Latvia

Introduction

The floating zone single crystal growth is an important technique for the preparation of single bulk crystals, well-known from the industrial production of high precision silicon especially for power electronics. The advantage of the method is the crucible-free processing of high reactive compounds where the melt zone is confined by the melt surface tension. Due to the large market of semiconductors, much attention was paid to the understanding of melt convection and the influence of external magnetic fields on the growth process of silicon single crystals and semiconductor compounds with well-known thermophysical properties. The research concentrates on the application of rotating magnetic fields [1, 2] or static magnetic fields [3] for the reduction of dopant fluctuations and time-dependent thermocapillary convection [4]. The understanding of heat transfer and fluid motion is needed in order to grow defect-free single crystals [5, 6].

In recent years, the single crystal growth of multicomponent intermetallics such as rare-earth-transition compounds became important. Silizides and borocarbides have been grown by this method to study the interesting magnetic, electric and transport properties as well as the superconductivity [7–9]. Problems in RF-floating zone crystal growth of high melting point compounds arise due to the strong heat radiation from the surface and melt convection resulting in a non-uniformly bent solid–liquid-interface with concave parts (towards the melt) in the surface region. Especially, complicated multicomponent intermetallic compounds are not producible as single crystals over the whole cross-section due to this unfavourable geometry of the zone. The aim of this work is the contact-less control of the heat and mass transfer during floating zone single crystal growth of intermetallic

compounds by well designed magnetic fields. The advantage of this method is the crucible-free processing of high reactive compounds and the flexible adjustment of the solid–liquid interface between crystal and melt.

High precision single crystals are greatly needed for the determination of interesting properties of novel materials. TiAl intermetallic alloys have been developed as potential materials for high temperature applications because of their excellent chemical and physical properties such as low density, high modulus and corrosion resistance at high temperatures. These characteristics are attractive for applications in aerospace and automotive industries [10, 11]. However, their low ductility at room temperature limits their application.

Experimental

Master alloys with the composition Ti45Al55 (at%), Ti40A60 (at%) were prepared from pure (99.99%, Alfa Aesar) Ti and Al in a cold crucible induction furnace under argon atmosphere and cast to rods with 6 mm diameter and 60 mm length. The cold crucible is made of several water-cooled copper sectors forming the container in which the alloy is processed. When reactive materials have to be manufactured with high purity, the cold crucible induction melting and casting method is the solution, because the copper crucible avoids any contamination of the material and the electromagnetic stirring of the melt provides excellent homogenisation of the melt. One feature is the combination of the alloying itself and subsequent casting in one temperature.

Single crystals of Ti45Al55 (at%) and Ti40A60 (at%) were grown by magnetic field controlled floating zone technique with induction heating in a vacuum chamber under argon atmosphere. A floating zone facility with 250 kHz generator frequency and 30 kW was used. The growth rate amounted to 10 mm/h. The rod rotation was selected to 10 rpm. The floating zone technique allows containerless crystal growth, necessary for high reactive materials with high melting temperatures such as TiAl alloys. Figure 1 shows the general schemes of the standard RF-floating zone and the two-phase coil system as well as their real experimental setups, respectively. In the standard FZ system, the flow is directed radially inwards at mid-height of the zone and has a typical double-vortex structure. The flow in the bulk of the zone is directed against the solid–liquid interface which leads to an unfavourable shape of the phase boundary with concave (from crystal melt) fringes at the outer rim of the crystal. The solution of forming a desired convex interface geometry developed here is to make use of the pumping effect if a secondary coil is added to the primary one (as shown in Fig. 1c, d), and if a phase shift is created between the two coils. The two coils with the induction coil geometry, placed opposite each other, form the two phase heater. The current in the secondary coil is induced by the RF-current of the primary coil [12].

The crystals were cut lengthwise and investigated by optical microscopy. For the investigation of the segregation behaviour, the composition of the sample was measured by electron probe microanalysis (EPMA).

Results and discussion

The important parameters to be adjusted in the two-phase stirrer system are inductance, capacitance and resistance of the secondary circuit, the phase shift of the coils and the distance between the two coils. In that way the fluid is pumped on its free surface from the primary to the secondary coil, and if this pumping is strong enough the double-vortex structure changes into a single vortex as shown in Fig. 2. This RF-two-phase stirrer provides a favourable flow field at the interesting solid–liquid phase boundary supporting a convex interface geometry. The strongest pumping effect with a single vortex structure is achieved if the phase shift between the coils is 90°. This is emphasised by the change of the dimensionless Reynolds number from 917 at 0° phase shift to 1160 at 60° phase shift and 1210 at 90° phase shift at a fixed parameter configuration. (Note, that the 0° phase shift flow pattern represents in the main the standard FZ double vortex structure.) The EM fields are calculated by solving the equations for the complex azimuthal component of the magnetic vector potential with a boundary integral method [13, 14]. The simulations of fluid flow and temperature distribution have been done using the commercially available code FLUENT. Hereby, all relevant terms such as buoyancy, Marangoni convection, electromagnetic forces, heat diffusion, crystal and feed rotation and the boundary conditions at the solid–liquid interface are considered. The EM force field generates a counter-clockwise meridional flow (the melt flows upwards along the free surface). The crystallization interface between the melt and the crystal is mostly convex.

Figure 3 presents the geometry of the solid–liquid interface of Ti45Al55 alloys grown with the two-phase heater. The sample in Fig. 3a was processed with 57° phase shift between the coils. Visible from the numerical simulation of the fluid flow pattern (Fig. 2b), a double vortex structure of the convection rolls at 60° coil phase shift is dominant where the melt is driven radial inwards at mid-height of the molten zone. As a result, the solid–liquid interface forms concave rims (see dotted line) leading to ingrowth of grains which inhibits single crystal

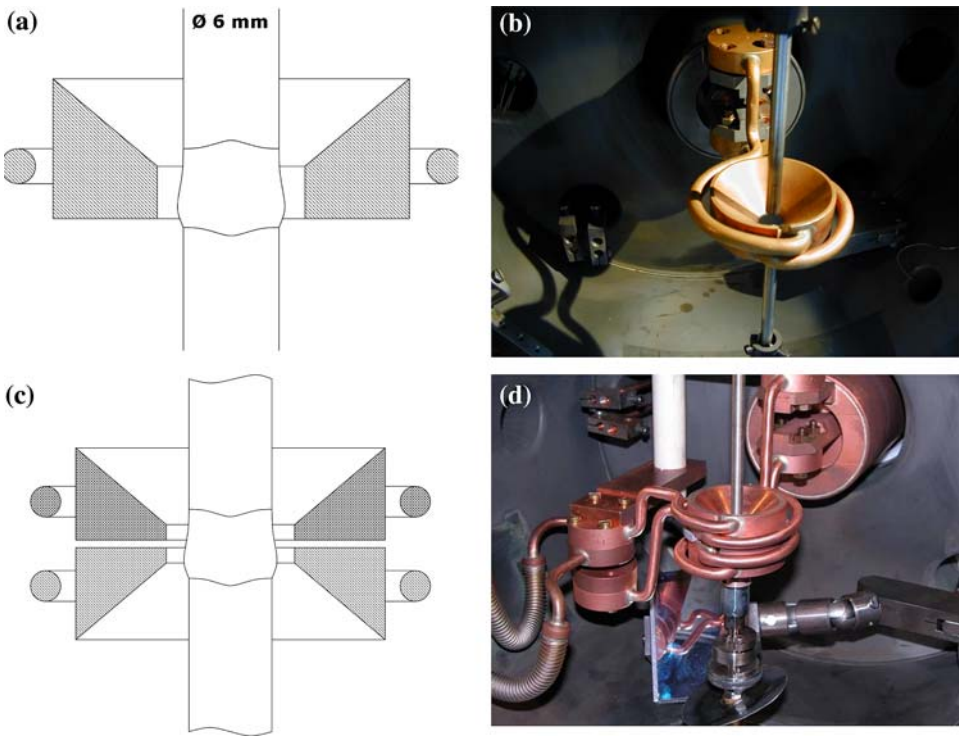

Fig. 1 *Left*: general scheme of standard FZ (**a**) and two-phase stirrer (**c**) crystal growth geometry. *Right*: Experimental setup of the standard (**b**) and two-phase stirrer system (**d**)

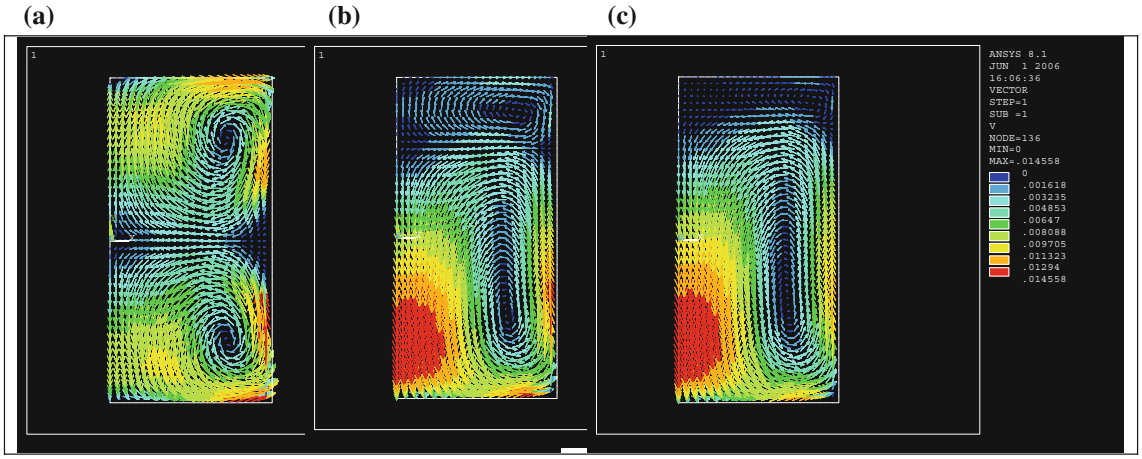

Fig. 2 *Streamlines*—transition from double vortex to single vortex structure, **a** 0°phase shift, $Re = 917$, **b** 60° phase shift, $Re = 1160$, **c** 90° phase shift, $Re = 1210$

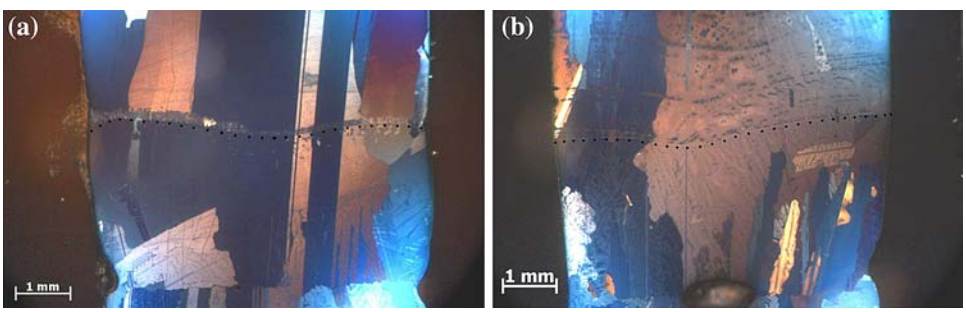

Fig. 3 Geometry of the solid–liquid interface (*black dots*) of Ti45Al55 alloys (longitudinal section of the zone), phase shift between primary and secondary coil **a** 57°, **b** 98°

growth over the full cross section (Fig. 3a). Contrariwise, a phase shift of 90° produces a single vortex flow structure (see numerical simulation, Fig. 2c) leading to a convex solid–liquid interface at all (dotted line), visible in the sample cross section of Fig. 3b. Such a convex solid–liquid interface enables the single crystal growth over the full cross section. Note that the polycrystalline crystals in Fig. 3 were grown only few millimetres in order to demonstrate growing in and growing out of crystals depending on unfavourable or favourable interface geometry. Moreover, due to the much stronger melt motion at 90° coil phase shift, cellular growth which would lead to constitutional supercooling is excluded (Fig. 3b).

Figure 4 shows the optical micrograph of another alloy with the composition Ti40Al60 processed at 90° coil phase shift. This sample was grown up to a length of 25 mm. The pictures are taken from attached regions starting with the melt on from the feed (Fig. 4a) till the final single crystal (Fig. 4d). The attention is here focused on the crystal growth where in Fig. 3 the solid–liquid interface with the adjacent solidified melt zone was brought into focus. Clearly visible from Fig. 4a–d, the grains grow rapidly out and leave a single crystal already after some millimetres.

Furthermore, the segregation behaviour from crystal to melt has been investigated by measuring the composition vertically through the solid–liquid interface using electron probe microanalysis (EPMA). Areas of 200 µm (horizontally) × 16 µm (vertically) were selected and adapted to each other over a distance of about 400 µm (vertically). Figure 5 shows the progression of Al concentration through the solid–liquid interface of a Ti40Al60 crystal grown under optimum convective conditions. As mentioned above, the flow pattern for 60° coil phase shift is dominated by a double vortex structure. The single vortex structure at 90° coil phase shift correlates with strong melt motion due to the

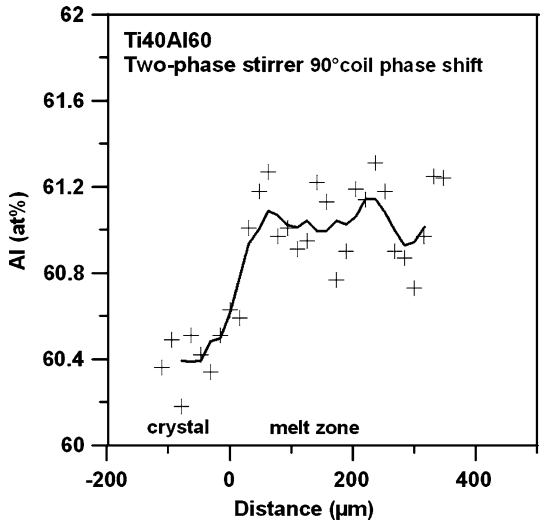

Fig. 5 Segregation behaviour measured on the Al concentration from crystal to melt for a Ti40Al60 alloy grown with 90° coil phase shift

enhanced electromagnetic pumping force obvious from the increased Reynolds number. It can be assumed that the strong melt motion assists the mixing of the alloying elements and reduces the diffusion boundary layer due to homogenisation ahead of the crystallisation front. The thickness of the diffusion boundary layer should be therefore diminished. During crystal growth of the TiAl compounds, typical segregation behaviour is observed leading to Al enrichment in the molten zone.

The concentration step at the solid–liquid interface for the grown Ti40Al60 single crystal (Fig. 4) is represented in Fig. 5 and displays a concentration rise from 60.4 at% Al in the single crystal to 61.04 at% Al in the liquid zone. These data are in good agreement with the newest phase diagram from Witusiewicz et al. [15], which displays a melt interval near 60% Al of less than 1 at%. It can therefore be derived that the optimum mixing of the melt by the two phase stirrer

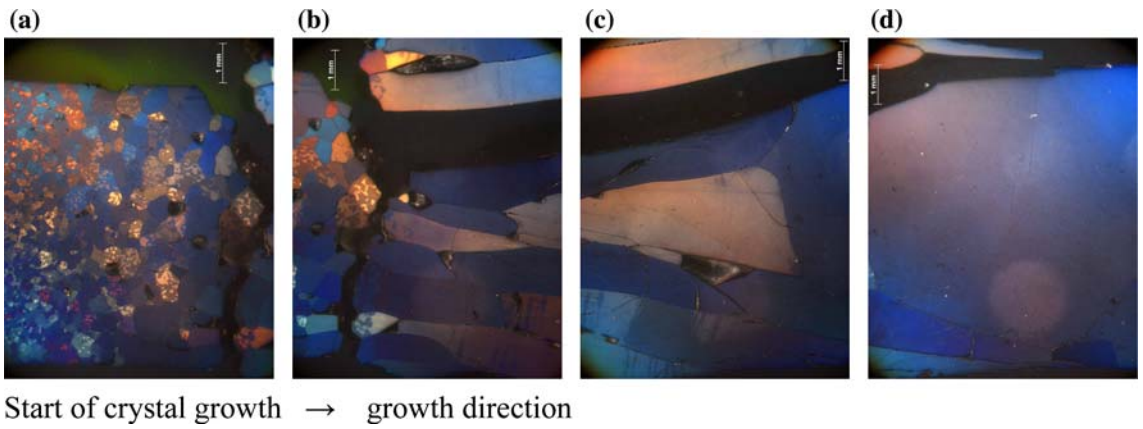

Fig. 4 Single crystal of a Ti40Al60 alloy, showing rapid growing out of grains, **a** start with polycrystalline feed rod, **b** and **c** grain growth, **d** single crystal almost at all

promotes a near equilibrium solidification behaviour without constitutional supercooling.

Conclusions

The radio frequency floating-zone growth with tailored magnetic two-phase stirrer system was applied to crystal growth of TiAl alloys. Depending on the parameter configuration of the system, mainly the phase shift between primary and secondary coil, the fluid flow structure passes from a double vortex to a single vortex structure at 90° phase shift. It creates a strong pumping force supporting the formation of the desired convex solid–liquid interface enabling the single crystal growth over the full cross section. The strong melt motion reduces the diffusion boundary layer due to the homogenisation ahead of the crystallisation front. The segregation behaviour from crystal to melt is in good agreement with the newest phase diagram from Witusiewicz et al. [15].

Acknowledgements The financial support of the Deutsche Forschungsgemeinschaft within the SFB 609 "Elektromagnetische Strömungsbeeinflussung in Metallurgie, Kristallzüchtung und Elektrochemie" is gratefully acknowledged.

References

1. Dold P, Cröll A, Lichtensteiger M, Kaiser Th, Benz KW (2001) J Cryst Growth 231(1–2):95
2. Ma N, Walker JS, Lüdge A, Riemann H (2001) J Cryst Growth 230(1–2):118
3. Cröll A, Benz KW (1999) Prog Cryst Growth Charact Mater 38(1–4):133
4. Passerone A, Eustathopoulos N (2005) J Mater Sci 40(9–10):XV. doi:10.1007/s10853-005-2128-z
5. Morthland TE, Walker JS (1997) Int J Heat Mass Transf 40(14):3283
6. Munakata T, Tanasawa I (1999) J Growth 206(1–2):27
7. Tanaka T, Bannai E, Kawai S, Yamane T (1975) J Cryst Growth 30:193
8. Takeya H, Habuta E, Kawano-Furukawa H, Ooba T, Hirata K (2001) J Magn Magn Mater 226–230(Part 1):269
9. Behr G, Löser W, Graw G, Bitterlich H, Freudenberger J, Fink J, Schultz L (1999) J Cryst Growth 198–199(Part 1):642
10. Clemens H (1995) Z Metallkd 86(12):814
11. Dimiduk DM (1999) Mater Sci Eng A 263:281
12. Hermann R, Behr G, Gerbeth G, Priede J, Uhlemann H-J, Fischer F, Schultz L (2005) J Cryst Growth 275:e1533–e1538
13. Priede J, Gerbeth G (2006) IEEE Trans Magn 42(2):301–308
14. Krauze A, Priede J, Hermann R, Gerbeth G (2008) Proceedings of the 7th PAMIR international conference on fundamental and applied MHD, Giens, 8–12 September 2008, pp 851–855
15. Witusiewicz VT, Bondar AA, Hecht U, Rex S, Velikanova TYa (2008) J Alloys Compd 465:64